ARTICLE

Ultrafast Proton Coupled Electron Transfer between Tryptophan and Tyrosine in Peptides Trp-Pro$_n$-Tyr

Haoyang Li[a], Simin Cao[b], Sanjun Zhang[a], Jinquan Chen[a*], Jianhua Xu[a*]

a. State Key Laboratory of Precision Spectroscopy, East China Normal University, Shanghai 200241, China
b. Key Laboratory of 3D Micro/Nano Fabrication and Characterization of Zhejiang Province, School of Engineering, Westlake University, Hangzhou 310024, China

(Dated: Received on December 30, 2022; Accepted on February 22, 2023)

A series of model peptides (Trp–Pro$_n$–Tyr, WP$_n$Y, n=0, 1, 2, 3, 5), which contain tryptophan (Trp, W), tyrosine (Tyr, Y), and proline (Pro, P), have been studied under three typical pH conditions (3, 7, and 10) by steady-state absorption and fluorescence spectroscopy, nanosecond time-resolved fluorescence and femtosecond time-resolved transient absorption spectroscopy. When the peptide's chain length is increased, Trp fluorescence quenching is expected to be gradually weakened. However, Trp fluorescence in WPY is strongly quenched and reveals even stronger quenching with increasing pH values, whose hypochromicity is clearly different from other model peptides. Transient absorption spectra also demonstrate that the excited state decay of WPY is much faster than that of other model peptides, especially at pH = 10. It is attributed to the efficient proton coupled electron transfer (PCET) between Trp and Tyr. Moreover, due to the very short distance between Trp and Tyr in WPY, this PCET process could be achieved by "direct transfer", contrasted with the slow and long-range PCET process in other model peptides. Our results of the dipeptides WY and WP further suggest that Trp may also have more complex interactions with the peptide backbone or proline in those peptides. This work provides an experimental evidence for the electron transfer mechanism in WY dyads, which can help ones to understand how to reduce Trp radicals in proteins.

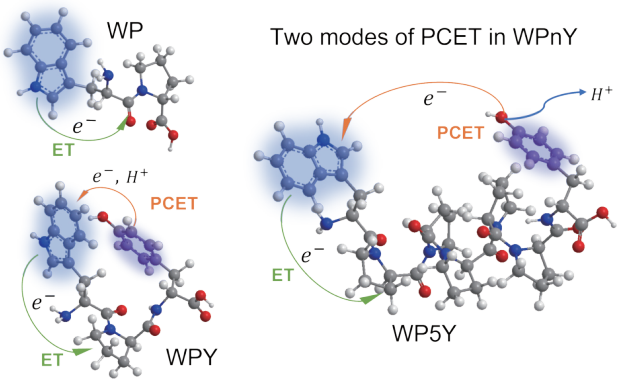

Key words: Proton coupled electron transfer, Tryptophan, Tyrosine, Peptides, Spectroscopy, Dynamics

I. INTRODUCTION

Among all the amino acids, tryptophan (Trp, W) with the highest extinction coefficient and fluorescence quantum yield, is the main ultraviolet (UV) absorbing group in proteins. As a naturally abundant biomolecule, Trp is a nontoxic and reliable "reporter" compared to the exogenous dye molecules and is highly sensitive to the local environment, therefore it has been widely used as a protein structure or microenvironment probe [1–3]. The fluorescence kinetics of Trp in peptides and proteins has been intensively studied, which have shown that even polypeptides or proteins containing single Trp usually exhibit the wavelength dependent multi-expo-

* Authors to whom correspondence should be addressed. E-mail: jqchen@lps.ecnu.edu.cn, jhxu@phy.ecnu.edu.cn

nential fluorescence decay. On nanosecond time scale, Trp fluorescence decay mainly results from its ground state heterogeneity, which can be caused by its "rotamer" positions or the complex environment of amino acid residues around Trp in proteins [4, 5]. On picosecond even femtosecond time scale, Trp fluorescence decay is reasonably explained by two kinds of theories: (i) ultrafast quenched conformation, also known as quasi-static self-quenching (QSSQ) [6–10]; (ii) bulk water and "biological water", the latter is also called slow solvent relaxation [11–14].

Tyrosine (Tyr, Y) has a lower extinction coefficient and fluorescence quantum yield than Trp, and the interaction between Tyr and Trp is of particular importance in proteins, which has been studied for years [15–23], including Förster resonance energy transfer (FRET) and electron transfer (ET). Recently, we employed femtosecond time-resolved up-conversion technique to perform an in-depth study of FRET between Tyr and Trp in model peptides Trp-Pro$_n$-Tyr (WP$_n$Y, n=0, 1, 2, 3, 5) [24]. The results indicated that ultrafast FRET from Tyr to Trp can severely affect the intrinsic fluorescence kinetics of Trp. It was also demonstrated that the peptide WPY provides the shortest distance between Trp and Tyr, which results in an ultrafast FRET lifetime of ~2 ps. In addition to FRET, we speculated that there may be other interactions between Trp and Tyr in those model peptides WP$_n$Y, such as electron transfer.

The electron transfer reaction between Tyr and Trp can find many important enzymatic and photobiological implications [18, 25–27], and help ones to understand the working mechanisms of numerous natural proteins or enzymes, for example, bovine serum albumin (BSA) [28], hen egg-white lysozyme [19, 29], nitrite reductase (in *Achromobacter cycloclastes*) [30] and ribonucleotide reductase (in *Escherichia coli*) [31]. The electron transfer accompanied by proton transfer, or the process in which both electrons and protons are transferred together, is usually called proton-coupled electron transfer (PCET) [32, 33]. Recent studies have proved that Tyr is a good PCET participant in peptides and proteins [34–38]. The phenol in Tyr can transfer electrons to the receptor simultaneously when removing protons. Especially in β hairpin [37], Barry *et al.* reported that free radicals can be scavenged through PCET between Tyr and Trp. It may protect proteins from the oxidative damage by reducing reactive oxygen species. Whereas this protection generally requires the formation of donor-receptor pairs or clusters, *i.e.*, Trp and Tyr should be in a small space, such as the pair consisting of Y122 and W48 in class 1a ribonucleotide reductases (*Escherichia coli* RNR) [36, 39]. Fortunately, those WY dyads are present in numerous enzymes or proteins, and play an important role in the electron/proton transport. It is known that, during ET or PCET, WY dyads can also realize the transfer of free radicals. Previous reports [40–42] have shown that free radicals can be transferred from the protein interior to the protein surface during the electron or proton transfer between aromatic amino acids. Subsequently, free radicals at the protein surface can be scavenged by cellular metabolism. Of course, this mechanism may further involve the quenching of reactive oxygen species.

Moreover, in previous work [43], the theoretical calculation of PCET between Trp and Tyr has been reported in detail. The results show that the direction of ET should be from Tyr to Trp because of lower energy barrier from Tyr to Trp, and the process of PCET may exist in two reactive forms (short-range and long-range) in peptides. Short-range PCET requires that the distance between Trp and Tyr is short enough to enable intermolecular contacts. In this case, a proton can be directly transferred from Tyr to Trp, further inducing the electron transfer. Whereas long-range PCET needs to be achieved with the aid of proton acceptors. Tyr can transfer a proton to a proton acceptor with a concomitant long-range electron transfer. This model has been validated in previous biomimetic peptide works [34, 35]. Although the study on PCET between Trp and Tyr has been extensive in peptides and proteins, the experimental evidence among them for the specific mechanism, and the distance dependence of PCET are still lacking. In this work, the model peptides WP$_n$Y are studied in detail by analysis of the fluorescence spectra, fluorescence lifetimes, and transient absorption spectra. The results found that there is the fastest radical recovery rate in the peptide WPY, regardless of pH conditions. In contrast, the recovery rates in other peptides are similar and do not show obvious distance dependence. This work provides an experimental evidence for the distance dependent nature of PCET to investigate the radical recovery of Trp in peptides, which might give particularly important guidance for understanding the PCET process between Trp and Tyr in proteins or enzymes.

DOI: 10.1063/1674-0068/cjcp2212181

II. MATERIALS AND METHODS

A. Steady-state absorption and fluorescence spectroscopy

The steady-state absorption spectra were recorded by a commercial UV-Vis spectrophotometer (TU1901, Beijing Purkinje General Instrument Co., Ltd.). The recording range was from 240 nm to 320 nm, and the step size was 1 nm. The fluorescence spectra were measured by FluoroMax-4 fluorescence spectrophotometer (Horiba) with 1 nm step size from 300 nm to 460 mm. We injected the sample into a fluorescent cuvette (2 mm) for the spectral measurement, and used the same cuvette for all measurements to remove the influence of cuvette on the spectra. All samples were freshly prepared before measurement. All measurements were made at 25 °C using the same instrument parameters. All data were measured repeatedly for 3 times, and the baseline and noise were removed.

B. Time-correlated single-photon counting system

The time-correlated single photon counting (TCSPC) system was home-built. The details of this instrument were introduced in previous work [44]. In short, a laser diode (PDL800-B, PicoQuant) was used to generate the picosecond pulses centered at 295 nm with the repetition rate of 10 MHz to excite the samples. The fluorescence detection system was composed of a time-correlated single photon counting module (PicoHarp300, PicoQuant) and a single photon counting photomultiplier tube (PMA165A-N-M, PicoQuant). A monochromator (7ISW151, Sofn Instruments) was used to select the appropriate wavelength for recording. The instrument response function (IRF) was determined to be ~500 ps by measuring Rayleigh scattering of 0.34 wt% SiO_2 nanoparticles in water. The measured decay data were fitted with a multi-exponential decay model, and the accuracy of fitting results was determined by the χ_R^2 value.

C. Femtosecond transient absorption spectroscopy

The femtosecond transient absorption (TA) setup was previously reported in detail [45]. We used a Ti:sapphire femtosecond laser system (Astrella, Coherent Inc.) to generate a fundamental beam at 800 nm (100 fs, 7 mJ, 1 kHz). The fundamental beam was divided into two beams, one entered an optical parametric amplifier (OPerA Solo, Coherent Inc.) and the other one entered TA system as the probe beam (white light continuum). The 295 nm pump beam generated by the optical parametric amplifier passed through an attenuation slice and used to excite the samples. In TA system, a commercial spectrometer (Helios fire, Ultrafast System) was used. The polarization between pump and probe beams was set at 54.7° (magic angle) to avoid the influence of anisotropy. The time resolution of TA system is ~120 fs. The sample was injected into a fused silica cell with an optical length of 2 mm. During the measurement, we placed a magnetic rod in the sample cell to continuously stir the sample solution. Igor software version 6.37 (Wavemetrics Inc., Portland, OR) was used to analyze the TA data.

D. Materials and samples

NaH_2PO_4 and Na_2HPO_4 were purchased from Aladdin (Shanghai, China), and directly dissolved in ultrapure water (18.2 MΩ·cm) without any purification to get the phosphate buffer (pH=7.2). Sodium hydroxide (NaOH) and phosphoric acid (H_3PO_4, >85%) were purchased from Sinopharm Chemical Reagent Co., Ltd. (Shanghai, China). Tryptophan was purchased from Sigma Aldrich.

All peptides (WP, WY, WPY, WP_2Y, WP_3Y and WP_5Y) were designed and synthesized by us in cooperation with Apeptide Co., Ltd. (Shanghai, China), and each peptide was purified (more than 98%) before use. Phosphate buffer was obtained by mixing NaH_2PO_4 and Na_2HPO_4 in ultrapure water. All samples were dissolved into the 10 mmol/L phosphate buffer (pH=7.2). High concentration sodium hydroxide solution and phosphoric acid were used to adjust the pH values of buffer solution. Finally, the pH value of solution was adjusted to 3.1 with acidic or 10.2 with alkaline, respectively. The concentration of 0.05 mmol/L for all samples was used to get their absorption spectra. The samples with the concentration of 0.2 mmol/L was used during the fluorescence spectra and TCSPC measurements. According to a previous report [46], we used the concentration of 3 mmol/L for TA measurements of all samples. All samples were freshly prepared before each experiment. After each test, we carefully checked the absorption and fluorescence spectra of the sample to ensure that the sample had no light-damage and photodegradation.

III. RESULTS AND DISCUSSION

A. Steady-state absorption and fluorescence spectra

FIG. 1 shows the absorption spectra and fluores-

DOI: 10.1063/1674-0068/cjcp2212181

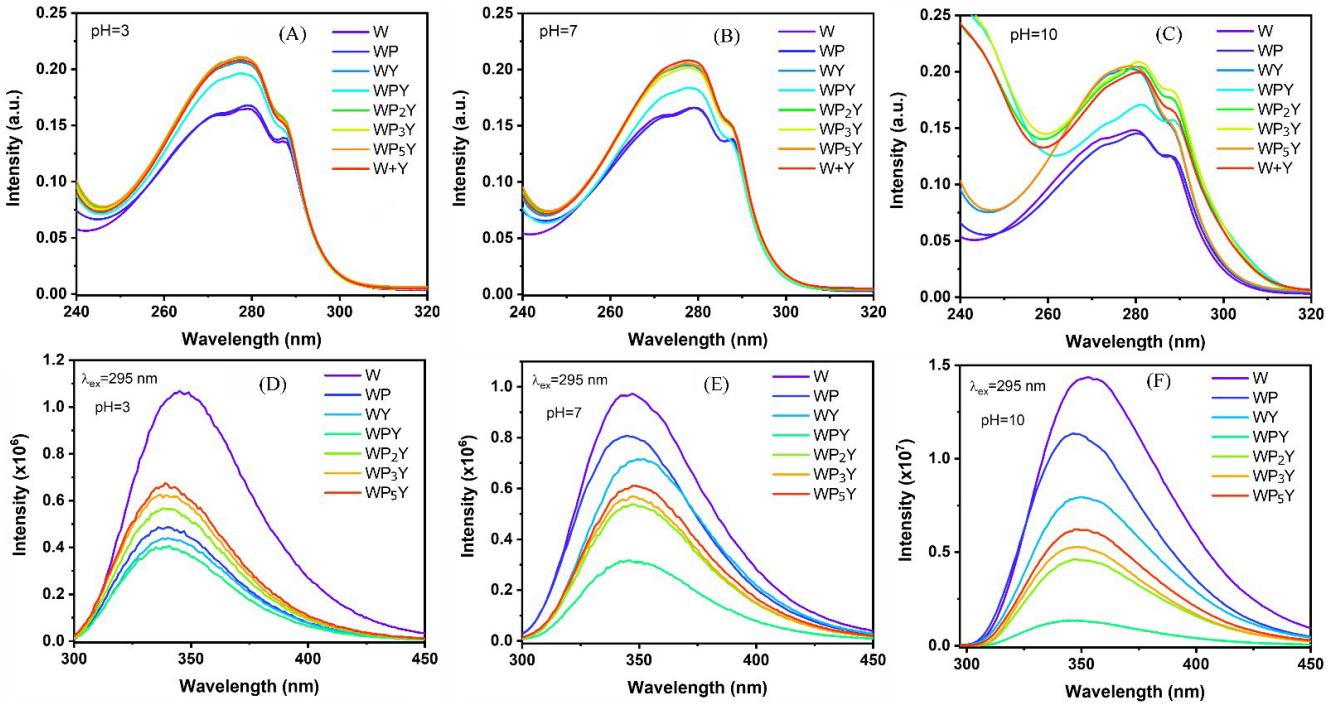

FIG. 1 Normalized absorption spectra (A, B, and C) and fluorescence spectra (D, E, and F) of W, WP, and WP$_n$Y (n=0, 1, 2, 3, 5) at three typical pH values (pH=3, 7, and 10). The excitation wavelength in the fluorescence spectra (D–F) is 295 nm.

cence spectra of W, WP, WY, WPY, WP$_2$Y, WP$_3$Y, and WP$_5$Y at three typical pH values (3, 7, and 10). The characteristic absorption bands of amino acids Trp and Tyr come from indole (~280 nm) and phenol (~275 nm), respectively. Obviously, when pH=3 and 7, the absorption spectra of W, WP and WP$_n$Y are similar. It should be noted that, since Trp and Tyr are included, the extinction coefficients of peptides WP$_n$Y should be higher than that of W and WP. The peptide WPY is expected to produce the similar results as other peptides WP$_n$Y. However, the extinction coefficient of WPY is slightly lower than that of other peptides WP$_n$Y. Moreover, this phenomenon is more obvious when pH=7. This hypochromism has been reported in previous nucleic acids, peptides or proteins [37, 47, 48], and the absorption spectra of W + Y (in FIG. 1(A, B, C)) can be used as a reference point to determine whether WP$_n$Y is hypochromic. This effect is usually attributed to the exciton coupling (dipole-dipole), dipole-induced dipole effect or electrostatic effect. This implies that the structure of peptide WPY is very different from that of other peptides WP$_n$Y, that is, the two ends of WPY may fold through complex interactions. This is consistent with the theoretical calculation results in our previous work [24] — WPY is more inclined to collapse. In WPY, the distance between W and Y becomes shorter so that the dipole-dipole interactions (or other effects described above) between the two aromatic rings occur. Further, this hypochromicity in WPY is more severe when the pH value is raised to 10. This suggests that WPY is more prone to form the "compact" structures with increasing pH value. Notably, at pH=10, all the absorption spectra of WP and WP$_n$Y change. WP, WPY, WP$_2$Y and WP$_3$Y show a slight red shift (1–3 nm), but WY and WP$_5$Y show no significant shift. Moreover, the spectral shapes of WPY, WP$_2$Y and WP$_3$Y are severely changed, a new absorption peak (~240 nm) appears on the blue side. These phenomena can be attributed to the fact that Y has a red shift of absorption in alkaline solution and the absorption peak of its S_2 state is shifted to the position of ~230 nm [49–51]. In addition, the change of energy levels due to the dipole-dipole interaction between W and Y is not excluded [36, 37]. These phenomena are similar to the previous results obtained in β hairpin peptides [37].

The fluorescence spectra of all samples were recorded in the range from 300 nm to 450 nm with the excitation wavelength of 295 nm (to avoid the influence of Tyr). At pH=7, the fluorescence spectra (FIG. 1(E)) of

DOI: 10.1063/1674-0068/cjcp2212181

W, WP and WP_nY are consistent with the results reported in previous work [24]. The emission peak of W is located at ~347 nm, while WY produces the reddest emission peak (~352 nm). The emission peaks of WP_nY all shift slightly due to the insertion of proline (P), for example, 345 nm for WP, 346 nm for WPY, 347 nm for WP_2Y, 347 nm for WP_3Y, and 348 nm for WP_5Y. As the number of P increases, the emission peak of WP_nY red shifts gradually. This can be attributed to the different charge distribution and hydrophobic properties [44]. In terms of fluorescence intensity, all the peptides have different degrees of fluorescence quenching compared to Trp itself. Different degrees fluorescence quenching of Trp usually occurs in peptides or proteins due to its different conformations, microenvironment changes, interactions with peptide chains or amino acids, *etc.* [6–8, 10, 44]. This also includes the quasi-static self-quenching (QSSQ) process of Trp. However, it is obvious that WPY has the strongest fluorescence quenching compared to other WP_nY peptides, and the integral of WPY is only 30.6% of W. WP has the smallest quenching, followed by WY. Whereas the peptides WP_2Y, WP_3Y, and WP_5Y are quenched to a similar extent with only minor differences ($WP_2Y > WP_3Y > WP_5Y$).

At pH=3 (FIG. 1(D)), the shape of Trp fluorescence spectrum does not change significantly (peak at ~347 nm) compared with that at pH=7. However, the fluorescence intensities of all samples have changed with varying degrees. The fluorescence intensities of WP and WY decrease significantly; that of WP_2Y basically unchanges; those of W, WP_3Y and WP_5Y slightly increase. The fluorescence emission peak of WY is ~341 nm, while the other peptides (WP, WPY, WP_2Y, WP_3Y and WP_5Y) are all around ~339 nm. Previous studies have shown that Trp in peptides is more susceptible to pH regulation than Trp itself, especially in the physiological pH range [52–55]. The amino groups ($-NH_2$) in acidic solution usually exist in the form of $-NH_3^+$ with a more efficient quenching ability than $-NH_2$ does. In addition, the structure and charge distribution of peptides are also important factors that can affect their fluorescence intensities [44]. Therefore, when the pH decreases, the degrees of fluorescence intensity change are different for different samples. Notably, the fluorescence intensity of WPY is still the lowest, only 34.9% of the integration of Trp fluorescence intensity. This ratio is elevated compared to that at pH=7. However, the fluorescence quenching of WPY is still bigger than other peptides at the same pH value.

Further, when the pH value is raised to 10 (FIG. 1(F)), the fluorescence intensity of Trp increases and its spectrum is red shifted (~353 nm). The spectral shape of WP has no changes compared with that at pH=7 (~345 nm). The fluorescence peaks of peptide WP_nY are similar (~348 nm), and WY is ~350 nm. In addition, the order of fluorescence intensity of all peptides is similar to that when pH=7 ($WPY < WP_2Y < WP_3Y < WP_5Y < WY < WP$). It should be noted that the fluorescence quenching of WPY is the strongest at pH=10, the integral of fluorescence intensity is only 8.6% of Trp. This shows that the fluorescence quenching degree of WPY increases with the increase of pH values. The special structure (folding) of WPY leads to an efficient quenching of Trp, which is the most efficient in alkaline solution. When the peptides WP_nY are in the solutions with pH=10, the part of phenol losts hydrogen ions to form YO^- (the pK_a value of phenol in Tyr is 10.64). Although the fluorescence emission spectrum of tyrosinate in alkaline solution is about 350 nm, however, compared with Trp, its extinction coefficient and fluorescence quantum yield are extremely low, thus it has no effect on the measurement of Trp fluorescence [56–60]. In WPY, the distance between W and Y is short, thus the influences of Y and YO^- on W become particularly important. In order to better understand the change of fluorescence characteristics of peptides WP_nY with pH values, we turn to the measurement of fluorescence lifetime.

B. Nanosecond resolved fluorescence spectra

Nanosecond time-resolved fluorescence decay curves (FIG. 2) of W, WP, WY and WP_nY were recorded by TCSPC at three typical pH values (excitation wavelength was 295 nm and detection wavelength was 350 nm). All the data are fitted, the resulting lifetime (τ_n) and amplitude (A_n) information are exhibited in Table I. The fluorescence decay curve of W can be fitted well with two lifetimes at all three typical pH values [52, 53]. However, at pH=7 and 10, W in the peptides requires three lifetimes for a good fit [44, 54, 55]. At pH = 3 (FIG. 2(A)), the fluorescence decay rates of all peptides are faster than that of W, and the good fits with only two lifetimes are available for all peptides and W. According to Table I, the average lifetime of W is 2.57 ns. WPY has the shortest average lifetime

DOI: 10.1063/1674-0068/cjcp2212181

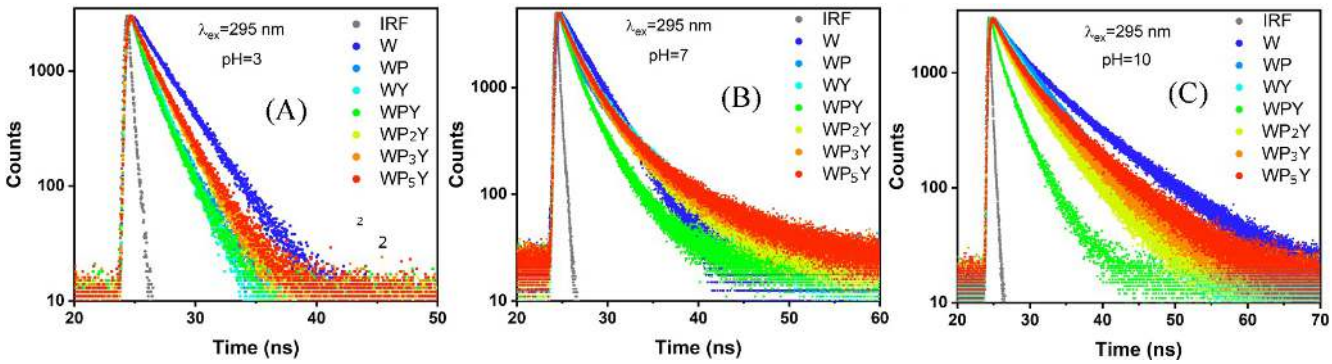

FIG. 2 Normalized nanosecond time-resolved fluorescence decay curves of W, WP, and WP$_n$Y (n=0, 1, 2, 3, 5) with pH=3 (A), 7 (B), and 10 (C). All fluorescence decay curves are excited at 295 nm.

TABLE I The lifetimes (τ_n in unit of ns) and amplitudes (A_n in unit of %) of W, WP, and WP$_n$Y (n =0, 1, 2, 3, 5) by fitting the decay curves obtained from TCSPC. The average lifetime (om TCSPC. The average lifetime (τ_{ave} in unit of ns) was also calculated.

Peptide	pH=3					pH=7							pH=10						
	A_1	τ_1	A_2	τ_2	τ_{ave}	A_1	τ_1	A_2	τ_2	A_3	τ_3	τ_{ave}	A_1	τ_1	A_2	τ_2	A_3	τ_3	τ_{ave}
W	28	0.45	72	2.71	2.57	5	0.40	95	2.90	–	–	2.88	42	2.49	58	8.28	–	–	7.24
WY	44	0.59	56	1.69	1.45	29	0.29	50	1.61	21	4.93	3.31	11	0.36	19	1.74	70	4.97	4.64
WP	68	0.40	32	2.01	1.53	61	0.35	29	2.25	10	6.06	3.50	11	0.59	69	4.32	20	7.53	5.32
WPY	61	0.32	39	1.73	1.40	56	0.22	32	1.35	12	3.27	2.00	56	0.20	25	1.42	19	3.36	2.42
WP$_2$Y	53	0.31	47	2.05	1.80	50	0.23	42	2.03	8	5.82	3.10	23	0.52	44	2.32	33	5.70	4.36
WP$_3$Y	52	0.30	48	2.06	1.82	55	0.24	39	2.10	6	6.80	3.33	16	0.37	46	2.24	38	6.43	5.09
WP$_5$Y	55	0.27	45	2.16	1.90	52	0.22	41	2.11	7	6.97	3.56	11	0.49	49	2.31	40	7.21	5.77

(1.40 ns), followed by WY (1.45 ns) and WP (1.53 ns). This is consistent with the results obtained from the steady-state fluorescence spectra and the extent of fluorescence quenching is the strongest for WPY. As the number of prolines increases, the length of peptide chain increases, and the average lifetime of peptides gradually increases (WP$_2$Y is 1.80 ns, WP$_3$Y is 1.82 ns, WP$_5$Y is 1.90 ns). This is a distance dependent phenomenon. In longer peptides, the quenching of W is weakened due to the increased distance between W and Y. However, this distance dependence is not strong. At pH=7 (FIG. 2(B)), all peptides except W require three lifetimes for a good fitting. Obviously, all the peptides have one more long-lifetime component (τ_3) than W. This can be attributed to the fact that the peptide has more complex charge distribution and conformation than W. Moreover, the lifetime component τ_1 occupancy of the peptides is much larger than that of W. This is consistent with previous observations in peptides where there are more rapid quenching pathways [7, 44]. According to Table I, WPY remains the shortest average lifetime (2.00 ns), and WP (3.50 ns) exhibits a longer average lifetime than WY (3.31 ns). With the insertion of proline (P), the average lifetime of polypeptides gradually increases (WP$_2$Y is 3.10 ns, WP$_3$Y is 3.33 ns, WP$_5$Y is 3.56 ns). This result is similar to that at pH=3. However, it is clear that the change of average lifetime with the increase of P number is more obvious at pH=7. Further, this phenomenon becomes more drastic when the pH increases to 10 (FIG. 2(C)). The lifetime of W gets longer in alkaline solvent, that of the peptides also does but by a lesser extent than W. However, only a slight increase occurs for the average lifetime of WPY (2.42 ns). And, the average lifetime increases gradually with the increase of peptide chain length (WP$_2$Y is 4.36 ns, WP$_3$Y is 5.09 ns, WP$_5$Y is 5.77 ns). The average lifetimes of WP$_n$Y (n=1, 2, 3, 5) increase with increasing the chain length no matter in acidic, basic or neutral solutions. This suggests that the number of prolines and the distance between W and Y are the two main factors affecting the fluorescence quenching of W in WP$_n$Y (n=1, 2, 3, 5). Furthermore, the effects of charge distribution and structural changes for W fluorescence quenching in WP$_n$Y (n=1, 2, 3, 5) are not excluded here. In particular, the average lifetimes of WP$_n$Y (n=1, 2, 3, 5) are more sensitive to the length of peptide chain in alkaline solutions. This indicates that the length of peptide chain is the dominant

DOI: 10.1063/1674-0068/cjcp2212181

factor for the fluorescence quenching of W in WPY in alkaline solution.

The average lifetime of WP (5.32 ns) is longer than that of WY (4.64 ns), the lifetime component τ_2 of WP has a higher ratio (A_2) than other peptides. It is noticed that the C-terminus of WP is P, while that of other peptides is Y. As a result, WP has different pK_a value, charge distribution, and conformation than the other peptides. Moreover, the reason why WPY has the shortest average lifetime is that the short lifetime (τ_1) is dominated. This indicates that there might be an ultrafast quenching pathway (<500 ps) in WPY at pH = 10.

In summary, the fluorescence decay curves confirm the results from the steady-state fluorescence spectra. WPY has the shortest fluorescence lifetime at three typical pH values, *i.e.*, its fluorescence is strongly quenched. The lifetimes of peptides gradually increase with the insertion of proline. The quenching of W in long peptides is weakened as the distance between W and Y is increased. Our previous work [24] has carefully investigated the structure and FRET (from Y to W) efficiency of WP_nY using the methods such as molecular dynamics simulations and experiments. The results showed that the distance between W and Y is 0.58 nm for WY, 0.56 nm for WPY, 0.90 nm for WP_2Y, 1.23 nm for WP_3Y, 1.70 nm for WP_5Y and 2.27 nm for WP_8Y, respectively. Obviously, the distance between W and Y in the dipeptide WY is longer than that in WPY. Thus, WY generally has longer average lifetime than WPY. However, at pH = 7 and 10, WY has longer average lifetime than WP_2Y has, which is unexpected. Moreover, the distance between W and Y in WP_2Y is much longer than that in WY. This indicates that the distance between W and Y in the peptides is not the only factor for fluorescence quenching of W. We do not rule out the effect of proline on the overall peptide charge distributions and conformations. To explore why WPY fluorescence is strongly quenched especially in alkaline solution, we turn to the measurement of transient absorption (TA).

C. Femtosecond transient absorption spectra

Femtosecond TA spectra of W, WY, WP, WPY, WP_2Y, WP_3Y and WP_5Y under 295 nm excitation are displayed in FIG. 3 (pH=3), FIG. 4 (pH=7), and FIG. 5 (pH=10), respectively. It is noted that the excitation wavelength is strictly controlled at 295 nm to avoid ultrafast energy transfer (FRET) between Tyr and Trp. This can effectively reduce the influence of FRET on the excited state absorption (ESA) signal of Trp [24]. A broad excited state absorption band from 320 to 640 nm appears for all samples. At pH=3, two peaks (350 and 425 nm) are clearly seen from the TA spectra of Trp (W) in FIG. 3(A). This is a typical characteristic of Trp photoproducts, which has been attributed to the partial protonation of Trp. Previous studies have shown that, two ESA bands centered at 350 nm and 425 nm are signatures of the photoproduct arising from S_1 quenching [46]. In addition, the negative contributions are expected from the stimulated emission (SE) at 300–400 nm and the ground state bleaches at $\lambda <$ 310 nm, respectively. Thus, these negative contributions might result in the decay dynamics of 350 nm peak different from that of 425 nm peak. It is noticed that the yield of Trp photoproducts is high in acidic solutions (pH=3), however, with increasing the pH values (pH=7 and 10), the generation of Trp photoproducts is gradually decreased. Further, previous studies have shown that Trp photoproducts could be a precursor of Trp triplet states [46, 61–63], and the superposition of Trp cation radical (580 nm) and neutral radical (510 nm) produces a broad band [64]. The generation of those protonated photoproducts causes the results that the signals of both radicals are gradually weakened, and an obvious isoabsorption point (~470 nm) appears. This indicates that those free radicals are gradually converted to the protonated photoproducts, and eventually this photoproducts could generate the triplet state species of W [46]. FIG. 3 shows that the generation of Trp protonated photoproducts is inhibited to various degrees in the peptides (WY, WP, WPY, WP_2Y, WP_3Y, and WP_5Y). Obviously, among all the peptides, the highest yield of Trp photoproducts is obtained in the dipeptide WY (FIG. 3(B)), and the photoproduct yield in the dipeptide WP (FIG. 3(C)) is lower than that of WY. This suggests that Pro could play an important role in inhibiting the Trp photoproducts (more potent than Tyr does). It is noted that the results for WPY (FIG. 3(D)) are basically similar to that for WP. In the acidic solution (pH=3), the inhibitory effect of Pro on the Trp photoproducts is dominant. However, this inhibitory effect is slightly weakened when the number of Pro is increased (WP_2Y in FIG. 3(E), WP_3Y in FIG. 3(F), and WP_5Y in FIG. 3(G)). This indicates that the inhibiting effect of photoproducts would slightly compromise with increasing the peptide's chain length. However, it is

DOI: 10.1063/1674-0068/cjcp2212181

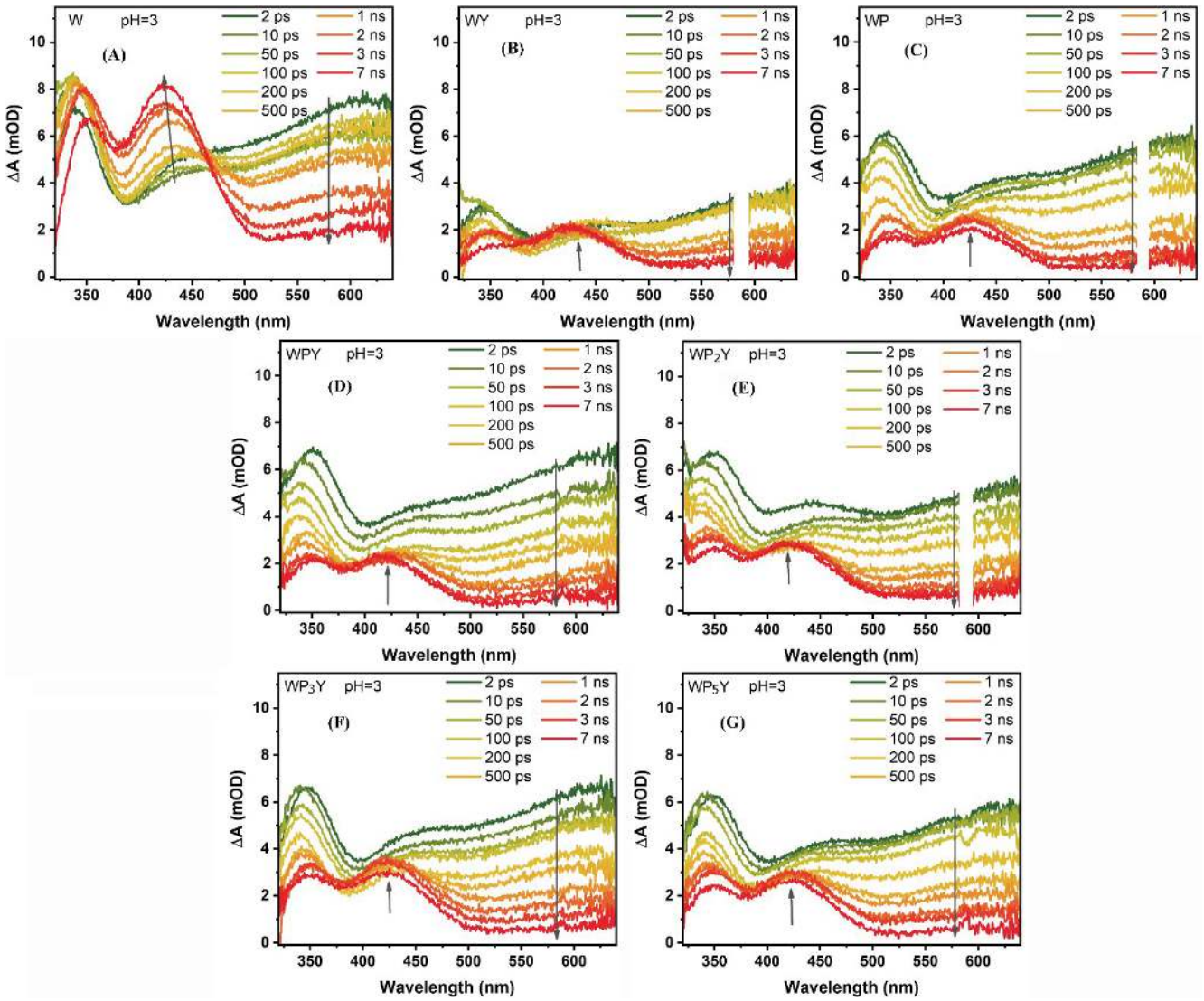

FIG. 3 Femtosecond TA spectra of W (A), WY (B), WP (C), WPY (D), WP$_2$Y (E), WP$_3$Y (F), and WP$_5$Y (G) at pH=3 with the excitation wavelength at 295 nm, respectively. Time window is from 2 ps to 7 ns.

worth noting that the decay of free-radicals is not suppressed but rather the decay rate is accelerated. This implies the existence of a "new process" to accelerate the free-radical recovery in the peptides. The radical species, which should be converted to Trp photoproducts, are greatly reduced by this "new process" in peptides.

When pH=7 (FIG. 4), the population of Trp photoproducts in either W (FIG. 4(A)) or other peptides decreases. Among all the peptides, the strongest inhibition effect on Trp photoproducts is found in WPY (FIG. 4(D)), followed by WP (FIG. 4(C)). In contrast, the signal of photoproducts in the dipeptide WY (FIG. 4(B)) is stronger than that in WP. The inhibition effect of Trp photoproducts is also gradually weakened with increase of the peptide's chain length (WP$_2$Y in FIG. 4(E), WP$_3$Y in FIG. 4(F) and WP$_5$Y in FIG. 4(G)).

When pH is increased to 10, the characteristic peak of Trp photoproducts at 425 nm is not obvious in FIG. 5(A). In alkaline solution (pH=10), the generation of such photoproducts would be greatly inhibited [46]. The excited state decay results for the dipeptides WY (FIG. 5(B)) and WP (FIG. 5(C)) are similar. The excited state decays of WP$_2$Y (FIG. 5(E)), WP$_3$Y (FIG. 5(F)) and WP$_5$Y (FIG. 5(G)) are similar, but obviously faster than that of the dipeptides WY and WP. Notably, the entire excited state spectrum of WPY (FIG. 5(D)) is undergoing a rapid decay. This decay process is much faster than that of all other peptides. This indicates that there is an ultrafast excited state quenching path-

DOI: 10.1063/1674-0068/cjcp2212181

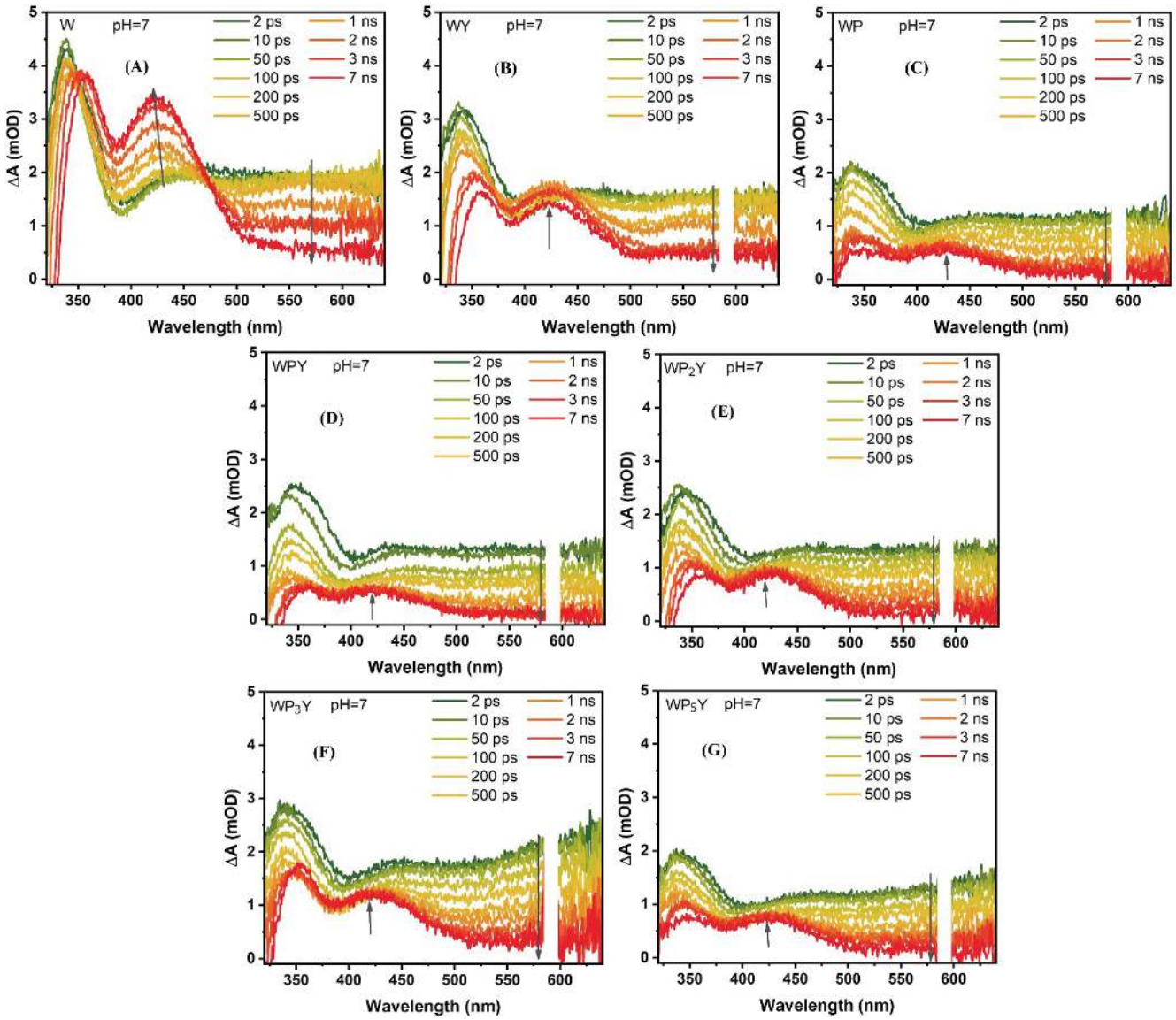

FIG. 4 Femtosecond TA spectra of W (A), WY (B), WP (C), WPY (D), WP_2Y (E), WP_3Y (F), and WP_5Y (G) at pH=7 with the excitation wavelength at 295 nm, respectively. Time window is from 2 ps to 7 ns.

way in WPY, which might be attributed to the interaction between Trp and Tyr. Moreover, this effect is pH dependent, and the strongest one is in alkaline solution (pH=10). This "new" excited state quenching pathway might be related to the ultrafast electron transfer between Trp and Tyr in WPY. This process greatly accelerates the recovery of Trp radicals, so that promotes the rapid decay of the entire excited state signal of WPY.

To more accurately grasp the decay process of Trp radicals, FIG. 6 presents the decay curves of the cation radical peak position (580 nm) under three typical pH values for all samples. The results of two-exponential fitting of all curves are presented in Table II. In the previous work [46], four lifetimes are used to describe the excited state kinetic decay process of Trp. These include the long-lifetime component of the triplet state (>40 ns) and the vibrational relaxation lifetime component (~1 ps). However, these two lifetime components are proportionally small for the time window of 7.5 ns. Therefore, we could fit the curves using only two exponentials. Previous work [37] in β hairpin peptides has also used this scheme with success. Further, we found that Trp could be well fitted with only one lifetime at pH = 10. Obviously, at pH = 3 (FIG. 6(A)), all peptides decay faster than Trp itself does. Although the decay curves are similar for all peptides, WPY has two lifetimes shorter than the other peptides does (125.9 ps and 3.2 ns). A slight distance dependence could be observed

DOI: 10.1063/1674-0068/cjcp2212181

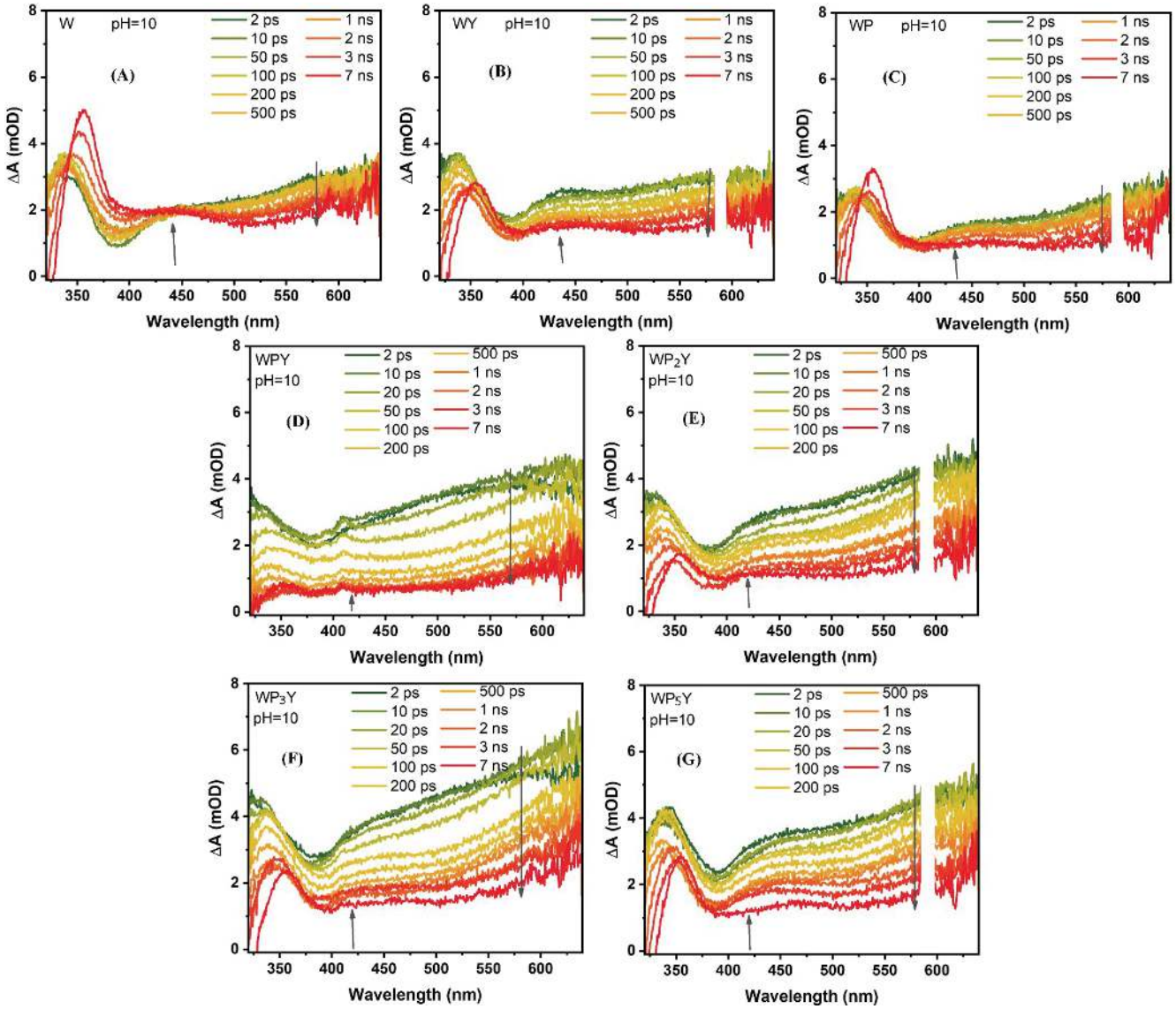

FIG. 5 Femtosecond TA spectra of W (A), WY (B), WP (C), WPY (D), WP$_2$Y (E), WP$_3$Y (F), and WP$_5$Y (G) at pH=10 with the excitation wavelength at 295 nm, respectively. Time window is from 2 ps to 7 ns.

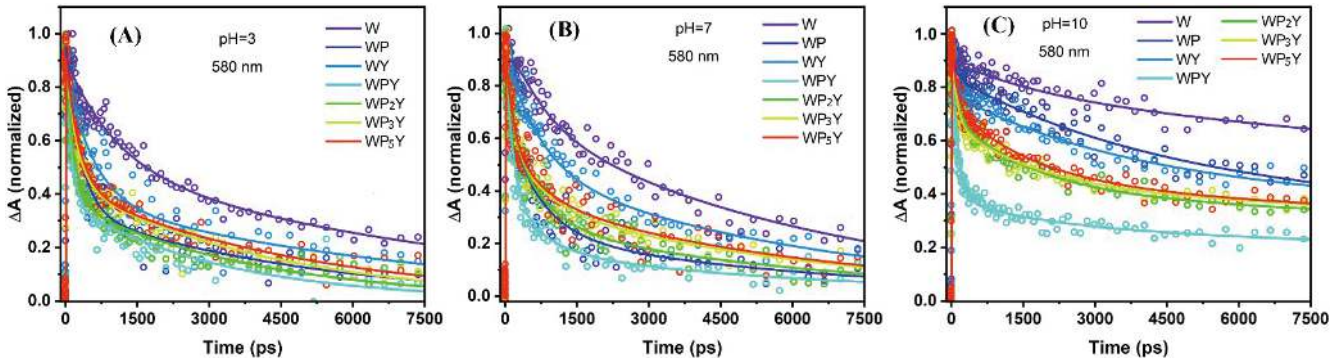

FIG. 6 Normalized femtosecond TA kinetics (at 580 nm) of W, WP and WP$_n$Y (n=0, 1, 2, 3, 5) with pH=3 (A), 7 (B) and 10 (C), respectively. The data collected by the TA system are represented by circles, and the fitting results are represented by lines.

DOI: 10.1063/1674-0068/cjcp2212181

TABLE II The lifetimes (τ_n in unit of ns) and amplitudes (A_n in unit of %) by fitting the decay curves obtained in FIG. 6.

Peptide	pH=3				pH=7				pH=10			
	A_1	τ_1	A_2	τ_2	A_1	τ_1	A_2	τ_2	A_1	τ_1	A_2	τ_2
W	43	1.03	57	8.43	50	2.57	50	6.98	100	12.30	–	–
WY	56	0.57	44	7.35	50	0.96	50	6.74	11	0.12	89	10.92
WP	64	0.30	36	4.94	69	0.37	31	6.54	19	0.11	81	11.87
WPY	58	0.126	42	3.22	64	0.15	36	2.59	59	0.08	41	9.54
WP_2Y	58	0.17	42	3.89	57	0.29	43	4.18	35	0.14	65	9.76
WP_3Y	50	0.23	50	4.23	54	0.25	46	5.00	37	0.12	63	11.13
WP_5Y	59	0.27	41	5.08	58	0.23	42	5.05	33	0.15	67	10.06

in peptides WP_2Y, WP_3Y and WP_5Y. The decay rate of cation radical characteristic peaks in WPY is accelerated with increasing pH values. An ultrafast decay appears in WPY when pH=10 (FIG. 6(C)), and the amplitude (59%) of this lifetime (87.9 ps) is significantly higher than that of the other peptides. This indicates that, in alkaline solution, there is an ultrafast radical recovery pathway in WPY. This is consistent with the inference from our TCSPC results. Obviously, the radical recovery rate of WPY is the fastest, and this process is exacerbated in alkaline solutions.

In previous work [36, 37, 43], PCET between Trp and Tyr was intensively studied in peptides. Studies have shown that when the distance between Trp and Tyr was close enough (~6 Å), Tyr could transfer one proton and simultaneously one electron to Trp, thus enabling Trp radical recovery. According to our previous work [24], the distance between Trp and Tyr in WPY is 5.6 Å. This distance satisfies the previously reported effective distance between Trp and Tyr, resulting in an efficient PCET effect. Additionally, both the steady-state and transient absorption spectra of WPY are similar to the results previously observed in β hairpin peptides [37]. Further, the radical recovery rate of WPY is pH dependent, which suggests that this process is related to the protons in solutions. Therefore, we speculate that this ultrafast radical recovery process in WPY might be attributed to the PCET between Trp and Tyr. It is noted that, in WPY, the spatial distance of Trp and Tyr is very short, so the PCET process might be a model of direct proton transfer [43]. Thus, the PCET process rate is even faster and more efficient. Meanwhile, in the peptides, Tyr could also make the PCET to Trp through water molecules and hydrogen bonds [37]. When the distance between Trp and Tyr is increased, Tyr would not be able to directly transfer the protons to Trp but transfer the protons to the solution or the proton acceptor in the peptide's chain followed by the long-range electron transfer process [43]. This process has been intensively studied in biomimetic peptides [34, 35]. It should be pointed out that the distance dependence on this long-range electron transfer is small. In other words, this long-range electron transfer is not very much related to the peptide's chain length, only related to the efficiency of proton transport. Thus, in this workr, it could be observed that the radical recovery rates of WP_2Y, WP_3Y and WP_5Y are almost the same. There is no strong distance dependence. This suggests that the PCET process (long range) in the long peptides is different from that in WPY. This process is only highly correlated with the concentrations of proton acceptors in solution and poorly correlated with the length of peptide's chain. Thus, this results in a large difference of free-radical decay curves between WPY and other peptides (two different PCET models). Moreover, for the dipeptides WY and YP, the free-radical recovery lifetime of WY is obviously longer than that of WP at pH = 3 and 7, but at pH = 10, the opposite result is observed. This indicates that WY achieves a faster radical recovery rate than WP does through the PCET process in alkaline solution. However, in neutral and acidic solutions, the PCET process of WY is inefficient and the radical recovery rate is slower than that of WP. It is noticed that the free radical recovery rate does not match the fluorescence lifetimes (from TCSPC). Therefore, we do not exclude that other complex quenching pathways in peptides may exist.

In summary, the transient absorption spectra of Trp and a series of peptides are investigated. At pH = 3 and 7, Trp photoproducts in peptides are inhibited with various degrees. This is due to the fact that the Trp photoproducts are pH sensitive [46]. And, the structure and

DOI: 10.1063/1674-0068/cjcp2212181

charge distribution of peptides also affect the yield of Trp photoproducts in peptides. Furthermore, the recovery rate of Trp radicals is clearly accelerated in the peptides. The PCET between Tyr and Trp is the dominant factor to accelerate the recovery rate of Trp radicals in peptides. And these phenomena are more obvious in WPY. When pH value is increased to 10, more efficient PCET occurrs due to the short distance between Trp and Tyr in WPY. This efficient free radical recovery pathway affects the whole excited state decay of WPY. Whereas the PCET in long peptides (WP_2Y, WP_3Y and WP_5Y) is found to be different from WPY. The long-range PCET process occurring in long peptides has low distance dependence, however, high correlation with the proton acceptor concentrations in solutions [34, 35]. Therefore, the long-range PCET process is stronger in the alkaline solutions. Furthermore, the contrast of WY and WP suggests that the interaction between Tyr and Trp is not solely responsible for Trp radical recovery, the effect of Pro on Trp excited state dynamics is also significant. This is probably achieved by the electron transfer. Moreover, this effect could also be attributed to the interactions with the peptide backbones. Trp radicals can be also decayed by the recombination with solvated electrons [48, 65].

IV. CONCLUSION

In this work, we found that the radical recovery rate of Trp could be accelerated in peptides. This might be attributed to the interactions between the peptide backbones (or amino acids) and Trp. The acceleration of Trp radical recovery rate results in a lower yield of Trp photoproducts, which in turn decreases the production of Trp triplet species. This could potentially protect proteins from the damage by reactive oxygen species [37]. Further, Trp radical recovery rate in WPY is the fastest, and these effects are the strongest in WPY, indicated with the appearance of hypochromism in the absorption spectrum of WPY and Trp fluorescence in WPY being strongly quenched. Especially at pH = 10, the whole excited state decay of WPY is accelerated due to the ultrafast PCET process between Trp and Tyr. However, the PCET mechanism of WPY may be different from the other peptides. Due to the shortest distance between Trp and Tyr in WPY, the efficient "direct" PCET might have occurred, while a long-range PCET process occurrs in other peptides. It is not excluded that other more complex interaction processes may exist. Thus, a careful QM-MM needs to be pursued in these model peptides. More experimental evidence should be provided for understanding those interactions, by which WY dyads could be used to protect proteins by reducing free radicals.

V. ACKNOWLEDGMENTS

This work was supported by the National Natural Science Foundation of China (No.11674101).

[1] C. R. Cantor and P. R. Schimmel, *Biophysical Chemistry: Part II: Techniques for the Study of Biological Structure and Function*, New York: Macmillan, (1980).
[2] P. R. Callis, *Methods in Enzymology*, Amsterdam: Elsevier, 113 (1997).
[3] J. R. Lakowicz, *Principles of Fluorescence Spectroscopy*, New York: Springer Science & Business Media, (2013).
[4] S. J. Kroes, G. W. Canters, G. Gilardi, A. van Hoek, and A. J. Visser, Biophys. J. **75**, 2441 (1998).
[5] M. Gonnelli and G. B. Strambini, Biophys. J. **104**, 155 (2003).
[6] J. Xu, T. Dmitri, K. J. Graver, R. A. Albertini, R. S. Savtchenko, N. D. Meadow, R. Saul, P. R. Callis, B. Ludwig, and J. R. Knutson, J. Am. Chem. Soc. **128**, 1214 (2006).
[7] J. Xu and J. R. Knutson, J. Phys. Chem. B **113**, 12084 (2009).
[8] J. Xu, J. Chen, D. Toptygin, O. Tcherkasskaya, P. Callis, J. King, L. Brand, and J. R. Knutson, J. Am. Chem. Soc. **131**, 16751 (2009).
[9] A. Biesso, J. Xu, P. L. Muino, P. R. Callis, and J. R. Knutson, J. Am. Chem. Soc. **136**, 2739 (2014).
[10] J. Xu, B. Chen, P. Callis, P. L. Muino, H. Rozeboom, J. Broos, D. Toptygin, L. Brand, and J. R. Knutson, J. Phys. Chem. B **119**, 4230 (2015).
[11] P. Jorge, P. Samir Kumar, and A. H. Zewail, Proc. Natl. Acad. Sci. USA **99**, 10964 (2002).
[12] S. K. Pal, J. Peon, and A. H. Zewail, Proc. Natl. Acad. Sci. USA **99**, 1763 (2002).
[13] S. K. Pal, J. Peon, and A. H. Zewail, Proc. Natl. Acad. Sci. USA **99**, 15297 (2002).
[14] D. Zhong, S. K. Pal, and A. H. Zewail, Chem. Phys. Lett. **503**, 1 (2011).
[15] G. Weber, Biochem. J. **75**, 335 (1960).
[16] G. Weber, Biochem. J. **75**, 345 (1960).
[17] R. F. Borkman and S. R. Phillips, Exp. Eye Res. **40**, 819 (1985).
[18] M. Faraggi, M. R. DeFelippis, and M. H. Klapper, J. Am. Chem. Soc. **111**, 5141 (1989).
[19] M. Weinstein, Z. B. Alfassi, M. R. DeFelippis, M. H. Klapper, and M. Faraggi, Biochim. Biophys. Acta

DOI: 10.1063/1674-0068/cjcp2212181

Prot. Struct. Mol. Enzymol. **1076**, 173 (1991).
[20] K. Bobrowski, J. Holcman, J. Poznanski, M. Ciurak, and K. L. Wierzchowski, J. Phys. Chem. **96**, 10036 (1992).
[21] A. K. Mishra, R. Chandrasekar, M. Faraggi, and M. H. Klapper, J. Am. Chem. Soc. **116**, 1414 (1994).
[22] K. Bobrowski, J. Poznański, J. Holcman, and K. L. Wierzchowski, J. Phys. Chem. B **103**, 10316 (1999).
[23] O. B. Morozova, R. Kaptein, and A. V. Yurkovskaya, J. Phys. Chem. B **116**, 12221 (2012).
[24] H. Li, G. Jiang, M. Jia, S. Cao, S. Zhang, J. Chen, H. Sun, J. Xu, and J. R. Knutson, Phys. Chem. Chem. Phys. **24**, 18055 (2022).
[25] J. Butler, E. J. Land, W. A. Prütz, and A. J. Swallow, Biochim. Biophys. Acta Prot. Struct. Mol. Enzymol. **705**, 150 (1982).
[26] C. Y. Lee, FEBS Lett. **299**, 119 (1992).
[27] J. Stubbe and W. A. van Der Donk, Chem. Rev. **98**, 2661 (1998).
[28] R. Joshi and T. Mukherjee, Biophys. Chem. **103**, 89 (2003).
[29] K. Bobrowski, J. Holcman, J. Poznanski, and K. L. Wierzchowski, Biophys. Chem. **63**, 153 (1997).
[30] K. Yamaguchi, K. Shuta, and S. Suzuki, Biochem. Biophys. Res. Commun. **336**, 210 (2005).
[31] J. M. Bollinger Jr., W. H. Tong, N. Ravi, B. H. Huynh, D. E. Edmondson, and J. Stubbe, J. Am. Chem. Soc. **116**, 8024 (1994).
[32] M. H. V. Huynh and T. J. Meyer, Chem. Rev. **107**, 5004 (2007).
[33] D. R. Weinberg, C. J. Gagliardi, J. F. Hull, C. F. Murphy, C. A. Kent, B. C. Westlake, A. Paul, D. H. Ess, D. G. McCafferty, and T. J. Meyer, Chem. Rev. **112**, 4016 (2012).
[34] B. Koronkiewicz, J. Swierk, K. Regan, and J. M. Mayer, J. Am. Chem. Soc. **142**, 12106 (2020).
[35] P. Li, A. V. Soudackov, B. Koronkiewicz, J. M. Mayer, and S. Hammes-Schiffer, J. Am. Chem. Soc. **142**, 13795 (2020).
[36] C. V. Pagba, T. G. McCaslin, G. Veglia, F. Porcelli, J. Yohannan, Z. Guo, M. McDaniel, and B. A. Barry, Nat. Commun. **6**, 10010 (2015).
[37] T. G. McCaslin, C. V. Pagba, S. H. Chi, H. J. Hwang, J. C. Gumbart, J. W. Perry, C. Olivieri, F. Porcelli, G. Veglia, and Z. Guo, J. Phys. Chem. B **123**, 2780 (2019).
[38] T. G. McCaslin, C. V. Pagba, H. Hwang, J. C. Gumbart, S. H. Chi, J. W. Perry, and B. A. Barry, Chem. Commun. **55**, 9399 (2019).
[39] P. Nordlund, B. M. Sjöberg, and H. Eklund, Nature **345**, 593 (1990).
[40] H. B. Gray and J. R. Winkler, Proc. Natl. Acad. Sci. USA **112**, 10920 (2015).
[41] J. R. Winkler and H. B. Gray, Philos. Trans. Royal Soc. A Math. Phys. Eng. Sci. **373**, 20140178 (2015).
[42] E. C. Minnihan, D. G. Nocera, and J. Stubbe, Acc. Chem. Res. **46**, 2524 (2013).
[43] X. Chen, L. Zhang, L. Zhang, J. Wang, H. Liu, and Y. Bu, J. Phys. Chem. B **113**, 16681 (2009).
[44] M. Jia, H. Yi, M. Chang, X. Cao, L. Li, Z. Zhou, H. Pan, Y. Chen, S. Zhang, and J. Xu, J. Photochem. Photobiol. B: Biol. **149**, 243 (2015).
[45] Y. Y. Liu, H. F. Pan, J. H. Xu, and J. Q. Chen, Chin. J. Chem. Phys. **34**, 621 (2021).
[46] J. Léonard, D. Sharma, B. Szafarowicz, K. Torgasin, and S. Haacke, Phys. Chem. Chem. Phys. **12**, 15744 (2010).
[47] H. DeVoe and I. Tinoco Jr., J. Mol. Biol. **4**, 518 (1962).
[48] A. M. a. Blanco-Rodríguez, M. Towrie, J. Sykora, S. Záliš, and A. Vlcek Jr., Inorg. Chem. **50**, 6122 (2011).
[49] C. V. Pagba, S. H. Chi, J. Perry, and B. A. Barry, J. Phys. Chem. B **119**, 2726 (2015).
[50] J. M. Antosiewicz and D. Shugar, Biophys. Rev. **8**, 151 (2016).
[51] E. Pieri, V. Ledentu, M. Huix-Rotllant, and N. Ferré, Phys. Chem. Chem. Phys. **20**, 23252 (2018).
[52] W. B. De Lauder and P. Wahl, Biochemistry **9**, 2750 (1970).
[53] D. M. Jameson and G. Weber, J. Phys. Chem. **85**, 953 (1981).
[54] L. Li, H. Yi, M. Chang, X. Cao, Z. Zhou, C. Qin, S. Zhang, H. Pan, Y. Chen, and J. Xu, Sci. Bull. **60**, 2129 (2015).
[55] L. Li, X. Cao, Z. Zhou, S. Zhang, H. Pan, J. Chen, and J. Xu, J. Appl. Spectrosc. **84**, 633 (2017).
[56] F. G. Prendergast, P. D. Hampton, and B. Jones, Biochemistry **23**, 6690 (1984).
[57] S. Pundak and R. S. Roche, Biochemistry **23**, 1549 (1984).
[58] K. J. Willis, A. G. Szabot, and D. T. Krajcarski, Photochem. Photobiol. **51**, 375 (1990).
[59] K. Willis and A. Szabo, J. Phys. Chem. **95**, 1585 (1991).
[60] J. Alexander Ross, W. R. Laws, K. W. Rousslang, and H. R. Wyssbrod, *Topics in Fluorescence Spectroscopy*, Boston: Springer, 1 (2002).
[61] Y. P. Tsentalovich, O. A. Snytnikova, and R. Z. Sagdeev, J. Photochem. Photobiol. A Chem. **162**, 371 (2004).
[62] D. Bent and E. Hayon, J. Am. Chem. Soc. **97**, 2612 (1975).
[63] K. L. Stevenson, G. A. Papadantonakis, and P. R. LeBreton, J. Photochem. Photobiol. A Chem. **133**, 159 (2000).
[64] J. Baugher and L. Grossweiner, J. Phys. Chem. **81**, 1349 (1977).
[65] S. Y. Reece, J. Stubbe, and D. G. Nocera, Biochim. Biophys. Acta Bioenerg. **1706**, 232 (2005).

DOI: 10.1063/1674-0068/cjcp2212181